EurJOC
European Journal of Organic Chemistry

Research Article
doi.org/10.1002/ejoc.202500278

Chemistry Europe
European Chemical Societies Publishing

www.eurjoc.org

Green Synthesis of Hantzsch Dihydropyridines from Biorenewable Furans Derived from Lignocellulosic Biomass

Gabriel Abranches Dias Castro,* Lorena Cristina de Andrade Leles, Eduardo Vinícius Vieira Varejão, Felipe Terra Martins, Paula Derksen Macruz, Eduardo Jorge Pilau, and Sergio Antonio Fernandes*

Hantzsch dihydropyridines constitute a class of N-heterocycles with significant pharmacological and technological applications. Due to their importance, the development of new sustainable synthetic methodologies for producing dihydropyridines is of great interest. This work presents the synthesis of dihydropyridines via the Hantzsch multicomponent reaction. Furanic aldehydes derived from lignocellulosic biomass are used as substrates, and *p*-sulfonic acid calix[4]arene ($CX4SO_3H$) is employed as an organocatalyst, under microwave irradiation (MWI). The furanic compounds are reacted with ethyl acetoacetate and ammonium acetate in the presence of 1.0 mol% of $CX4SO_3H$ for 10 min at 80 °C under MWI. Twenty one dihydropyridines are synthesized in yields ranging from 43% to 96%. Two dihydropyridines are obtained as crystals suitable for X-ray diffraction analysis, and their crystallographic data are provided. Moreover, the catalytic system can be reused for seven reaction cycles without significant yield loss. The developed methodology offers numerous advantages. It enables the production of dihydropyridines from renewable substrates via a multicomponent reaction in a single step, with a short reaction time. The process uses a reusable organocatalyst and eliminates the need for solvents or metal catalysts.

1. Introduction

Hantzsch dihydropyridines are a class of six-membered *N*-heterocycles, first synthesized in 1881 by the German chemist Arthur Rudolf Hantzsch.[1,2] Following their pioneering synthesis, these molecules remained largely unstudied for nearly a century, until structural and functional similarities were recognized between the dihydropyridine scaffold and the reduced forms of nicotinamide adenine dinucleotide phosphate (NADH and NADPH).[3–5] Since then, the development of synthetic methodologies and the investigation of the medicinal properties of substituted dihydropyridines as well, have garnered significant interest from various research groups.[3,4,6]

These studies have significantly advanced medicinal chemistry, leading to the development of a class of calcium channel blockers (CCBs) widely used in clinical settings for the treatment of several cardiovascular diseases, including hypertension and angina.[7] The chemical structures of the principal dihydropyridine CCBs are shown in **Figure 1**.[8–12] Furthermore, it has been reported that dihydropyridines have a series of other pharmacological and technological activities of great importance and interest to society.[13]

The Hantzsch pyridine reaction is a well-established method for the synthesis of dihydropyridines.[3,14] It involves a straightforward and rapid four-component reaction in which an aldehyde reacts with two equivalents of a β-ketoester and a nitrogen donor (e.g., an ammonium salt).[3,7] As a multicomponent reaction, this method allows the desired products to be obtained in a single step, eliminating the need for successive purification processes and reducing the excessive use of solvents. These features are in line with the principles of green chemistry, by facilitating the synthesis of target compounds using low-toxicity reagents, minimizing waste, reducing environmental impacts, and safeguarding human health.[15,16]

By varying the structures of the aldehyde and the β-ketoester, the Hantzsch reaction enables the synthesis of a wide range of substituted dihydropyridines, with many studies reporting the use of benzaldehyde and its derivatives as starting materials.[3,7] In the present work, we report the implementation of the Hantzsch multicomponent for the synthesis of a series of dihydropyridines using furfural (FF), 5-hydroxymethylfurfural (HMF), and other furanic compounds derived from lignocellulosic

G. A. D. Castro, L. C. A. Leles, E. V. V. Varejão, S. A. Fernandes
Grupo de Química Supramolecular e Biomimética (GQSB)
Departamento de Química, Universidade Federal de Viçosa
Universidade Federal de Viçosa
Viçosa, MG 36570-900, Brazil
E-mail: gabriel.a.castro@ufv.br
santonio@ufv.br

F. T. Martins
Instituto de Química
Universidade Federal de Goiás
Goiânia, Goiás 74001-970, Brazil

P. D. Macruz, E. J. Pilau
Laboratório de Biomoléculas e Espectrometria de Massas, Departamento de Química
Universidade Estadual de Maringá
Maringá, Paraná 87020-900, Brazil

Supporting information for this article is available on the WWW under https://doi.org/10.1002/ejoc.202500278

Research Article
doi.org/10.1002/ejoc.202500278

Chemistry Europe
European Chemical Societies Publishing

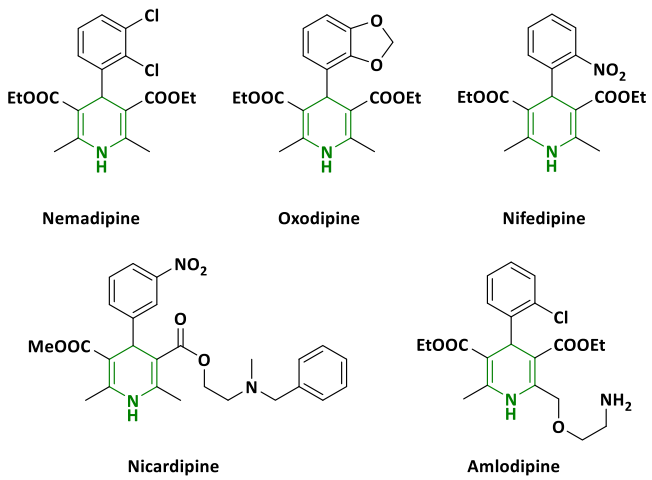

Figure 1. Some commercial dihydropyridine derivatives used as medicines for cardiovascular diseases (dihydropyridine ring is highlighted in green).

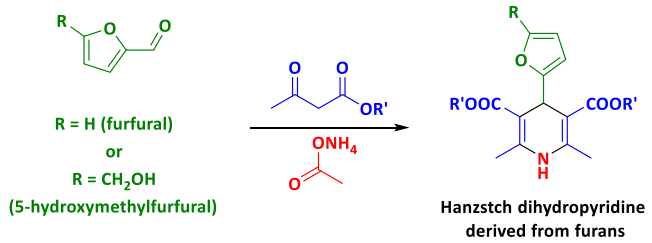

Figure 2. Synthesis of Hantzsch dihydropyridines from FF and HMF derived from lignocellulosic biomass.

biomass[17–20] (**Figure 2**). These compounds are important renewable and sustainable substrates, obtained from the dehydration of five- and six-carbon monosaccharides that are constituents of the polymeric chains of cellulose and hemicellulose. They have a significant potential to replace chemical building blocks currently derived from fossil resources.[20–24]

Furthermore, FF and HMF can undergo structural modifications including esterification,[25,26] etherification,[27] alkylation,[28] and direct arylation.[29,30] These modifications result in a variety of derivatives that can also be utilized for the synthesis of dihydropyridines and other chemical classes[17,18] (Figure 2).

Guided by the principles of green chemistry, the present work aims to evaluate the use of FF and its derivatives obtained from renewable lignocellulosic biomass, in the synthesis of dihydropyridines through the Hantzsch multicomponent reaction,[16] employing *p*-sulfonic acid calix[4]arene ($CX4SO_3H$) as an organocatalyst. The $CX4SO_3H$ is a supramolecule of the calix[*n*]arenes class, initially studied by David Gutsche.[31] Calix[*n*]arenes are macrocycles constructed from phenols, linked together by methylene bonds in the ortho to hydroxyl positions. The size of these macrocycles can vary from 3 to 20 phenolic units, and the "*n*" in their nomenclature represents the number of these units.[31] The investigation of $CX4SO_3H$ as an organocatalyst for Hantzsch reaction was motivated by previous successful results obtained by our research group in a variety of chemical transformations,[32–39] including multicomponent reactions.[40–46] Indeed, $CX4SO_3H$ displays several chemical characteristics that enhance its performance as an organocatalyst, including good thermal and chemical stability, noncorrosiveness, recyclability, low volatility, and low toxicity.[43,46,47]

2. Results and Discussion

2.1. Evaluation of the Effect of Time, $CX4SO_3H$ Amount, and Temperature

Initially, the effect of reaction time on the yield of dihydropyridine **D1** (**Table 1**, entries 1–8) was evaluated, with other reaction conditions fixed at 70 °C, microwave irradiation (MWI), and using 2.00 mol% of $CX4SO_3H$ as the organocatalyst. FF, ethyl acetoacetate, and ammonium acetate were employed as model substrates in a molar ratio of 1:2:2, respectively. The experiments were conducted solvent-free to minimize waste generation.[16] The results indicated that the yield of dihydropyridine **D1** increased with time, reaching a maximum at a reaction time of 10 min (Table 1, entries 1–5). On extending the reaction time beyond 10 min (Table 1, entries 5–8), no significant change in the yield of dihydropyridine **D1** was observed. Consequently, 10 min was established as the optimal reaction time for the synthesis of dihydropyridine **D1**.

Subsequently, the effect of the $CX4SO_3H$ organocatalyst amount on the reaction yield was examined (Table 1, entries 5, 9, and 10). It was found that using $CX4SO_3H$ in amounts greater than 1.00 mol% did not enhance the reaction yield. Conversely, a significant decrease in yield was noted when the reaction was conducted with only 0.5 mol% of $CX4SO_3H$ or in the absence of the organocatalyst (Table 1, entries 11 and 12). Therefore, 1.00 mol% $CX4SO_3H$ was selected for the synthesis of dihydropyridine **D1**.

Next, the effect of temperature on the yield of dihydropyridine **D1** was evaluated (Table 1, entries 10 and 13–16). It was observed that the yield of dihydropyridine increased with rising temperature, achieving a maximum yield of 96.6% at 80 °C (Table 1, entry 15). At higher temperatures (Table 1, entry 16), no further improvement in reaction yields was noted. Therefore, 80 °C was established as the optimal temperature for the synthesis of dihydropyridine **D1**. Consequently, the best conditions for the synthesis of dihydropyridine **D1** were determined to be 10 min, 1.00 mol% $CX4SO_3H$, and 80 °C, utilizing MWI (Table 1, entry 15). These conditions were subsequently tested under conventional heating (CH) using an oil bath instead of MWI. It was observed that conducting the reaction under CH resulted in a significantly lower yield (Table 1, entry 17).

The substantial difference in the yield of **D1** observed between the MWI and CH experiments (Table 1, entries 15 and 17, respectively) can be attributed to the distinct energy transfer mechanisms employed by each heating method. MWI provides more energy-efficient heating by directly applying microwave energy to molecules and ions, leading to a rapid temperature rise due to ionic conduction and dipole rotation. In contrast, CH involves a combination of heat transfer through convection and conduction, resulting in a slower rate of heating.[48,49]

Research Article
doi.org/10.1002/ejoc.202500278

Chemistry Europe
European Chemical Societies Publishing

Table 1. Optimization of the reaction time, organocatalyst ($CX4SO_3H$) amount and temperature.

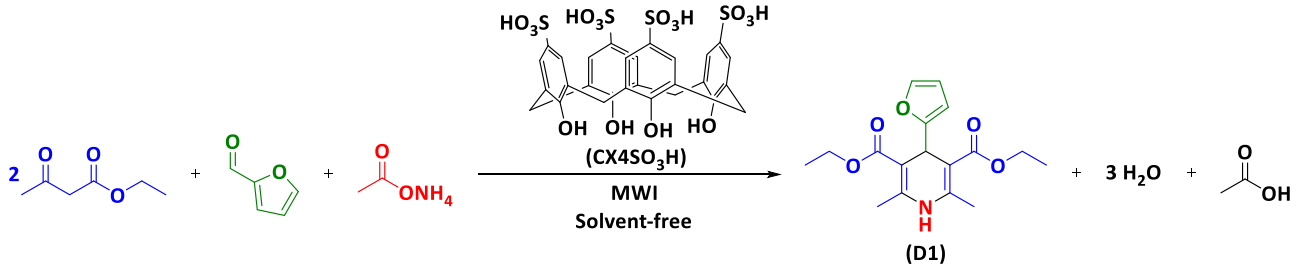

Entry	Time [min][a]	$CX4SO_3H$ [mol%]	Temperature [°C]	Yield of D1 [%][b]
1	1.00	2.00	70	30.5 ± 2.1
2	2.50	2.00	70	58.9 ± 0.2
3	5.00	2.00	70	74.5 ± 0.0
4	7.50	2.00	70	85.5 ± 1.0
5	10.00	2.00	70	92.7 ± 1.5
6	15.00	2.00	70	93.7 ± 0.2
7	20.00	2.00	70	91.6 ± 0.5
8	30.00	2.00	70	92.7 ± 1.5
9	10.00	3.00	70	91.7 ± 0.7
10	10.00	1.00	70	92.6 ± 2.2
11	10.00	0.50	70	53.8 ± 0.2
12	10.00	0.00	70	49.5 ± 2.5
13	10.00	1.00	50	53.6 ± 0.2
14	10.00	1.00	60	66.7 ± 0.0
15	10.00	1.00	80	96.6 ± 1.0
16	10.00	1.00	90	91.9 ± 2.5
17[c]	10.00	1.00	80	32.0 ± 2.7

[a]Reagents and conditions: 1.0 mmol of FF, 2.0 mmol ammonium acetate, 2.0 mmol ethyl acetoacetate, and MWI reactor. [b]Yield was determined by standard (dihydropyridine **D1**) calibration curve GC–MS analysis and the error calculated through preparing the samples in triplicate. [c]Experiments performed with CH in an oil bath.

2.2. Comparison of the Catalytic Activity of $CX4SO_3H$ with Other Acids

The catalytic activity of $CX4SO_3H$ was compared with that of other commercial acid catalysts (hydrochloric acid, sulfuric acid, and *p*-toluenesulfonic acid [PTSA]). In all experiments involving the various acid catalysts, the molar amounts of H^+ were kept constant, and the same reaction conditions previously established were employed. It was observed that the use of all three acid catalysts resulted in lower yields compared to those obtained with $CX4SO_3H$ (**Figure 3**). A plausible explanation for this phenomenon could be the unique encapsulation capabilities of $CX4SO_3H$, which may facilitate the formation of host–guest systems stabilized by intermolecular interactions, such as π–π interactions, hydrophobic interactions, and hydrogen bonding. These interactions may stabilize reaction intermediates, thereby enhancing the catalytic activity.[41,43,50,51]

Furthermore, the use of $CX4SO_3H$ is recommended due to its low toxicity and noncorrosiveness, unlike the mineral acids studied, which generate hazardous and corrosive waste.[25,52] It is noteworthy that the yield observed with H_2SO_4 (65.3%) was significantly lower. This reduction in yield can be attributed to the degradation of FF caused by the presence of this highly corrosive acid. Such degradation was evidenced by the formation of a black precipitate upon acid addition, indicating the generation of humins.[25,52]

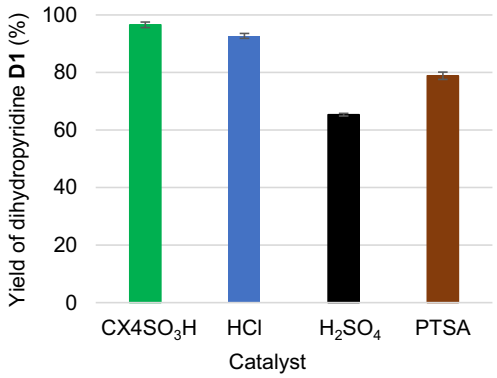

Figure 3. Comparison of $CX4SO_3H$ with other acid catalysts. The concentration of H^+ was kept constant (4.0 mol%). *Reagents and conditions*: 1.0 mmol of FF, 2.0 mmol ammonium acetate, 2.0 mmol ethyl acetoacetate, MWI reactor (100 W), 80 °C and 10 min.

Research Article
doi.org/10.1002/ejoc.202500278

2.3. Evaluation of Other Furanic Aldehydes as Substrate

After establishing the optimal conditions for the synthesis of dihydropyridine **D1** (10 min, 1.0 mol% of $CX4SO_3H$, and 80 °C) using FF as the starting material, the scope of the reaction was extended by evaluating different furanic aldehydes as substrates. As illustrated in **Figure 4**, 21 dihydropyridines (**D1**–**D21**) were synthesized, with yields ranging from 43% to 96%. It is important to highlight that seven of these dihydropyridines (**D7**, **D8**, **D9**, **D18**, **D19**, **D20**, and **D21**) were synthesized for the first time in this study. Overall, no clear correlation was observed between the reaction yields and the substitution patterns on the furan ring.

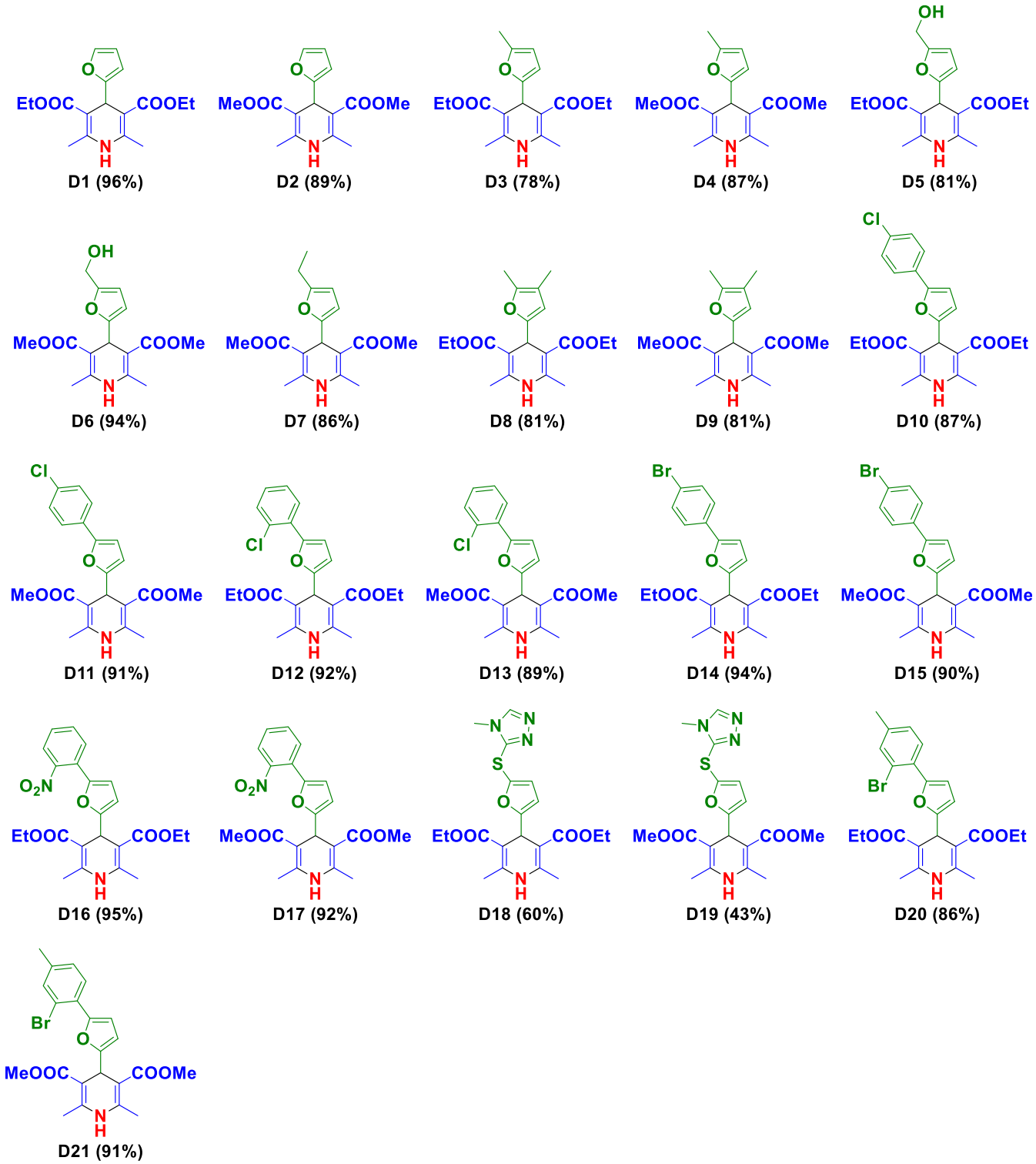

Figure 4. Scope of the reaction with different aldehydes, employing $CX4SO_3H$ as organocatalyst. Yields calculated for the isolated compounds.

Research Article
doi.org/10.1002/ejoc.202500278

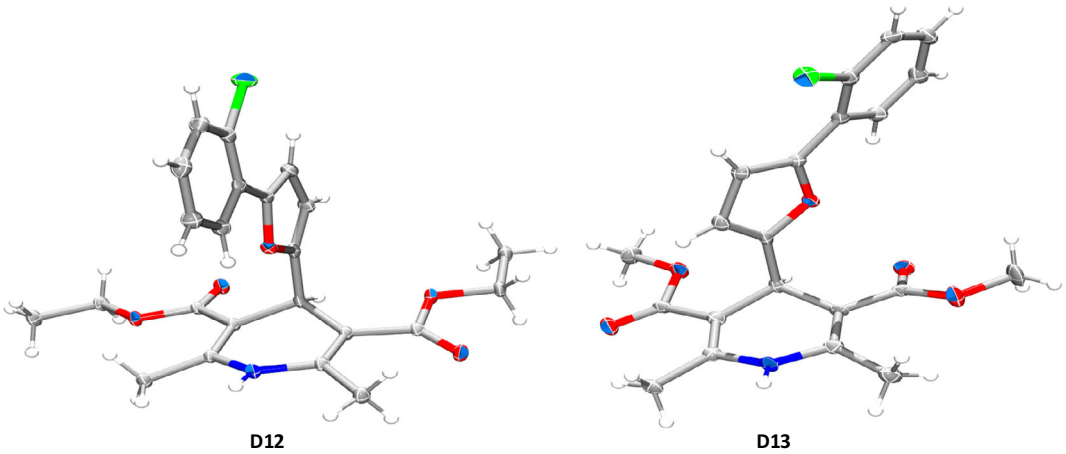

Figure 5. View of the chosen asymmetric unit of dihydropyridines **D12** and **D13** with nonhydrogen atoms represented by their corresponding ellipsoids with 50% probability.

Single crystals of dihydropyridines **D12** and **D13** were obtained for structural elucidation through X-ray diffraction experiments, which successfully confirmed their molecular structures (**Figure 5**). Compound **D12** crystallized in the triclinic space group $P\bar{1}$, containing only one molecule per asymmetric unit (Figure 5). In contrast, compound **D13** crystallized in the monoclinic space group P21/n, also with only one molecule per asymmetric unit (Figure 5).

2.4. Reuse of the Catalyst

Seeking a more sustainable and economically viable process, the possibility of reusing the organocatalyst was evaluated.[15,16] After the synthesis of dihydropyridine **D1** under the previously established reaction conditions (1.0 mol% $CX4SO_3H$, 10 min, and MWI heating at 80 °C), the organocatalyst was precipitated using ethyl acetate, separated by centrifugation, and oven-dried for reuse in a subsequent reaction cycle. This process was repeated five more times, with the supernatant analyzed by gas chromatography–mass spectrometry (GC–MS) for quantification of dihydropyridine **D1**. As shown in **Figure 6**, the yield of dihydropyridine **D1** remained consistently above 90% during the first four cycles. However, in the seventh reuse cycle, the yield decreased slightly by 86%. This minor decrease in yield may be attributed to material loss during the catalyst recovery, with an 80% recovery rate observed after seven cycles. The ^{1}H nuclear magnetic resonance (NMR) of the recovered organocatalyst (Figure S93, Supporting Information) indicated that its chemical structure remains intact. Thus, the ability to recover and reuse the catalyst without compromising its chemical integrity contributes to a more sustainable process, reducing waste generation.[15,16]

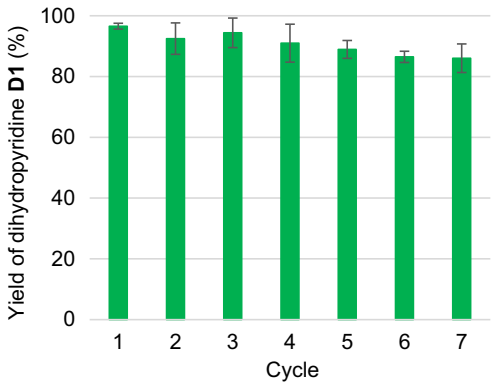

Figure 6. Dihydropyridine **D1** yields in organocatalytic reuse cycles. *Reagents and conditions*: 1.0 mmol of FF, 2.0 mmol ammonium acetate, 2.0 mmol ethyl acetoacetate, MWI reactor (100 W), 80 °C and 10 min.

2.5. Comparison of the Methodology Developed for the Synthesis of Dihydropyridine D1 with Literature Reports

Different methodologies for the synthesis of dihydropyridine **D1** from FF have been recently reported. A summary of the reaction conditions and yields obtained for **D1** in each of these studies is presented in **Table 2**. It can be observed that the method developed in the present work (Table 2, entry **1**) achieved **D1** at yields comparable to or higher than those obtained in other studies. The present methodology was carried out under milder conditions, requiring less reaction time, lower catalyst loading, and the use of renewable raw materials, while minimizing both solvent consumption and waste generation. For instance, in 2021, El-Remaily et al. reported an 83% yield of dihydropyridine **D1** using a heterogeneous manganese (III)-porphyrin complex (10 mol%) as the catalyst in water under reflux at 100 °C for 80 min[53] (Table 2, entry **2**). Similarly, Bakhtiarian and Khodaei synthesized **D1** with an 87% yield using a magnetic nanocomposite catalyst based on pectin modified with disulfonic acid (Fe_3O_4-Pec-DSA) (36.5 wt%) in ethanol, under ultrasound at 40 °C for 30 min[54] (Table 2, entry **3**). Additionally, Shaibuna and Sreekumar achieved a 92% yield using a deep eutectic solvent (DES) composed of $ZrOCl_2.8H_2O$ and ethylene glycol, with stirring at room temperature for 25 min[55] (Table 2, entry 4). Overall, in all those works, the synthesis of **D1** required longer reaction times,

Research Article
doi.org/10.1002/ejoc.202500278

Table 2. Comparison of the reaction conditions and yield for the synthesis of dihydropyridine **D1** in different works.

Entry	Solvent	Catalyst [Amount]	Conditions	Yield [%]	Ref
1	Solvent-free	$CX4SO_3H$ (1.0 mol% = 8.4 wt%)	MWI, 80 °C, 10 min	96	This work
2	Water	5,10,15,20-tetrakis-(4-sulfonatophenyl)-porphyrin manganese (III) chloride (10 mol%)	CH, reflux (100 °C), 80 min	83	[53]
3	Ethanol	Fe_3O_4-Pec-DSA (36.5 wt%)	CH, ultrasonic, 40 °C, 30 min	87	[54]
4	DES ($ZrOCl_2.8H_2O$/ethylene glycol (1:2))	–	Room temperature, 25 min	92	[55]
5	Solvent-free	Halloysite nanotubes-functionalized sulfonic acid (104 wt%)	CH, 60 °C, 60 min	92	[56]
6	Ethylene glycol	Ascorbic acid (20 mol%)	MWI, 80 °C, 3 min	80	[57]
7	Ethanol	Coconut endocarp shell ash (10 wt%)	Room temperature, 18 min	88	[58]
8	Ethanol	Cu/Cu_2O@g-C3N4 (10.4 wt%)	5 watt white LED lamp, room temperature, 51 min	91	[59]
9	DES (choline chloride and ammonium acetate)	–	CH, 120 °C, 10 min	91	[60]
10	Solvent-free	1,4-diazabicyclo[2.2.2]octanium diacetate (25 mol%)	CH, 80 °C, 180 min	97	[18]
11	Water	Gluconic acid (25 mol%)	CH, 60 °C, 180 min	70	[17]

use of solvents and metal catalysts, and afforded **D1** in lower yields compared to the methodology presented here (Table 2, entries 1–4).

In 2022, Gupta et al. obtained **D1** in a yield of 92% using halloysite nanotubes functionalized with sulfonic acid (104 mol%) as a catalyst at 60 °C under CH for 60 min[56] (Table 2, entry 5). That methodology required six times longer than the approach presented in the present work, and approximately 12 times more catalyst mass (Table 2, entries 1 and 5). Ray et al. reported the synthesis of **D1** under MWI at 80 °C for 3 min, using ethylene glycol as solvent and ascorbic acid (20 mol%) as catalyst, obtaining **D1** in 80% yield[57] (Table 2, entry 6). That method required the use of a solvent and significantly larger quantities of catalyst compared to the approach proposed in this work, while still providing **D1** in lower yields.

In another study, Patil et al. obtained dihydropyridine **D1** in 88% yield using coconut endocarp shell ash as the catalyst (10 wt%) in ethanol at room temperature for 18 min[58] (Table 2, entry **7**). In 2023, Singh et al. employed a heterogeneous photocatalyst made of doped copper graphitic carbon nitride and copper oxide (Cu/Cu_2O@g-C3N4) to synthesize dihydropyridine **D1**.[59] They achieved a yield of 91% with a catalyst amount of 10.4 wt%, using an LED lamp as a radiation source, ethanol as a solvent, and a reaction time of 51 min at room temperature (Table 2, entry 8). This methodology also involved the use of a solvent and a metal catalyst, requiring approximately five times longer than the conditions established in this study (Table 2, entries 1 and 8).

Kumar et al. prepared dihydropyridine **D1** with 91% yield using a DES (choline chloride plus ammonium acetate) at 120 °C under CH for 10 min[60](Table 2, entry **9**). Bhat et al. reported a 97% yield for dihydropyridine **D1** using the ionic liquid 1,4-diazabicyclo[2.2.2]octanium diacetate (25 mol%) as the catalyst at 80 °C under CH for 180 min[18] (Table 2, entry **10**). This method not only required a solvent and significantly longer reaction time, but also involved the use of an ionic liquid, which is less favorable due to higher costs and potential toxicity (Phuong et al., 2010). Finally, Anchan et al. prepared dihydropyridine **D1** with a 70% yield using a substantial amount (25 mol%) of gluconic acid as catalyst in water at 60 °C under CH for 180 min[17] (Table 2, entry 11).

2.6. Contribution to the Knowledge on the Hantzsch Reaction Mechanism

The mechanism of the Hantzsch multicomponent reaction is complex and has been extensively discussed in the literature. Various pathways involving different intermediates and steps have been proposed. In 1986, Katritzky et al. investigated the mechanism using ammonia, benzaldehyde, and three β-dicarbonyl compounds as model reactants. They suggested that the most likely pathway involves the reaction of benzaldehyde with a β-dicarbonyl compound, leading to the formation of a chalcone. Simultaneously, ammonia reacts with another β-dicarbonyl compound to produce an enamine. The rate-limiting step is believed to be a Michael addition between the chalcone and the enamine, followed by cyclization to yield the dihydropyridine.[61] Further studies have indicated that additional pathways are also plausible. In 2014, Santos et al. examined the Hantzsch reaction mechanism, discussing five potential pathways. By intercepting and identifying intermediates, they provided evidence that the reaction can proceed through three convergent pathways, all leading to the formation of Hantzsch dihydropyridine.[62] **Figure 7** illustrates these three possible paths (**A**, **B**, and **C**), considering the reagents employed in the present work (ammonium acetate, two equivalents of ethyl acetoacetate, and FF). The three proposed pathways (**A**, **B**, and **C**) involve the following: **Path A**; the chalcone (intermediate 2), formed from aldol condensation

Research Article
doi.org/10.1002/ejoc.202500278

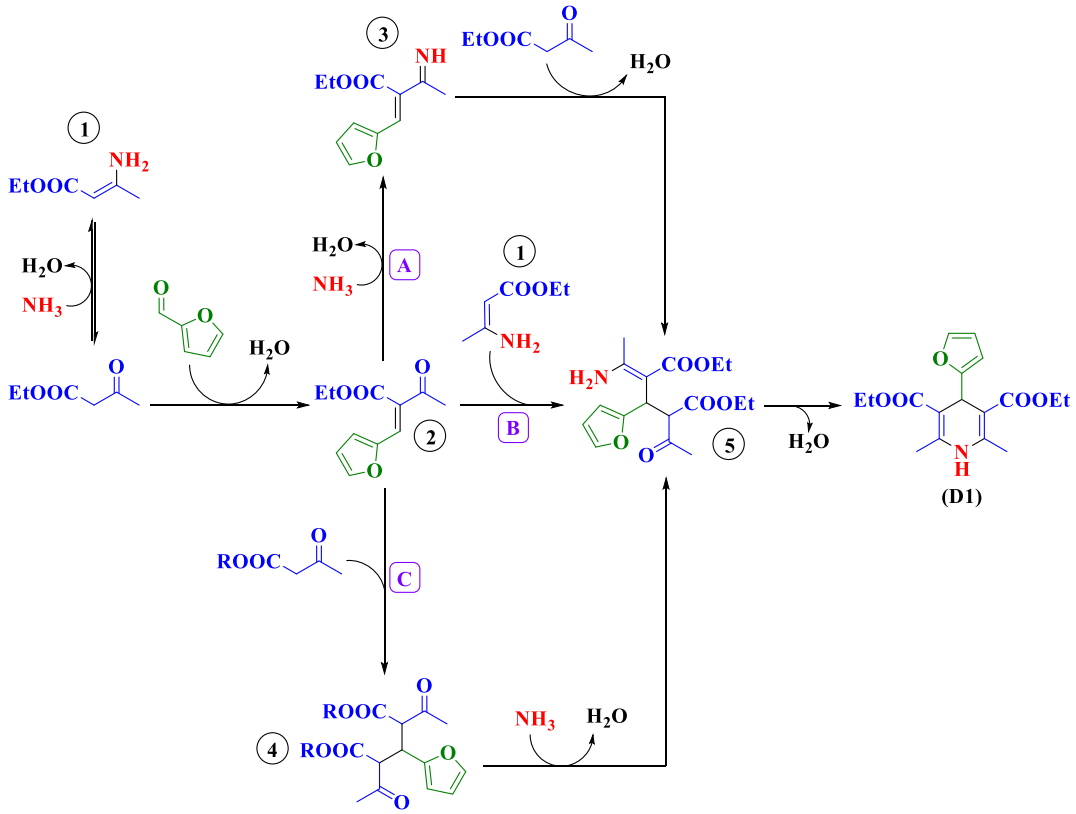

Figure 7. Paths of the Hantzsch reaction (**A**, **B**, and **C**) to obtain dihydropyridines proposed by Santos et al.[62]

between the aldehyde and β-ketoester, reacts with ammonia to create an imine (intermediate 3). This imine then reacts with another equivalent of the β-ketoester to form the Michael adduct (intermediate 5). **Path B** proposed by Katritzky et al., involves a Michael addition between the enamine (intermediate 1) and the chalcone (intermediate 2). **Path C** involves the reaction of the chalcone (intermediate 2) with a second equivalent of the β-ketoester to produce intermediate 4, which then reacts with ammonia to yield the Michael adduct (intermediate 5). These pathways highlight the intricate nature of the Hantzsch multicomponent reaction and the various mechanisms that can lead to the desired product. It is important to emphasize that, in the present work, $CX4SO_3H$ acts as a catalyst in all reaction stages. For this, it acts as a Bronsted acid and donates protons. These protons decrease the activation energy to access the reaction intermediates and consequently, increase the reaction rate.[63]

GC–MS analysis of the reaction mixtures from the multicomponent reaction revealed peaks corresponding not only to the dihydropyridine **D1** and the reactants (FF and ethyl acetoacetate), but also to various reaction intermediates. As shown in **Figure 8**, the chromatogram displays peaks for the (*E*/*Z*) isomers (*m*/*z* 208), formed by the aldol condensation between FF and one equivalent of ethyl acetoacetate, as well as the enamine (*m*/*z* 129) generated from the reaction of ammonia (produced in situ from ammonium acetate) with ethyl acetoacetate. Additionally, peaks corresponding to the two isomeric (*E*/*Z*) imines (*m*/*z* 207), resulting from the reaction of ammonia with the Michael addition product, were also detected. The mass spectra for all

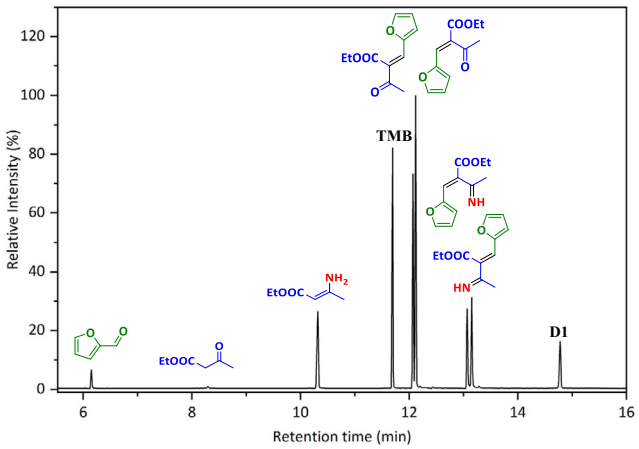

Figure 8. Chromatogram (GC–MS) of the Hantzsch multicomponent reaction mixture.

identified peaks are provided in the Supplementary Material (Figure S94–S101, Supporting Information). These findings support and corroborate two of the three proposed pathways (**A** and **B**) outlined by Santos et al. and illustrated in Figure 7, confirming the complexity of the reaction mechanism involved in the synthesis of dihydropyridine **D1**.[62]

Thus, the present work also provides evidences for previously proposed synthetic pathways for the Hantzsch reaction, contributing to consolidating the mechanism proposed by Santos et al. and Katritzky et al.[61,62]

Research Article
doi.org/10.1002/ejoc.202500278

3. Conclusion

A more sustainable and ecofriendly methodology for synthesizing dihydropyridines using substrates derived from lignocellulosic biomass has been developed. This method employs $CX4SO_3H$ as an organocatalyst (1.0 mol%) under MWI at 80 °C for just 10 min. A total of 21 dihydropyridines were synthesized using various furanic aldehydes, with yields ranging from 43% to 96%, including three compounds reported for the first time. Compared to several recently reported methods, our approach demonstrates comparable or even superior yields, achieved through solvent-free reactions, rapid reaction times, and without the need for metal catalysts. Additionally, we confirmed that the catalyst can be recovered and reused for up to seven cycles with minimal loss of efficiency. Overall, this synthetic methodology presents potential for sustainable chemical processes, as it aligns with several principles of green chemistry, including waste prevention, atom economy, synthesis using low-toxicity reagents, use of renewable raw materials, reduction of solvents and auxiliaries, energy efficiency through heating via MWI, avoidance of derivatization processes for analysis and synthesis, catalysis, and the prevention of accidents through safe chemical processes.

4. Experimental Section

Materials

All solvents and reagents used were of high purity, as recommended by the manufacturers (Merck or Sigma-Aldrich) for synthesis and/or chemical analysis.

Instruments

The synthetic procedures were carried out under MWI using a CEM Discovery reactor and 10 mL Pyrex glass tubes. The temperature was monitored by an internal probe. GC–MS analyses were performed using a SHIMADZU GCMS-QP201 °C Ultra mass spectrometer. NMR spectra were obtained on a Varian Mercury 300 MHz spectrometer operating at 300 MHz for ^1H and 75 MHz for ^{13}C, or on a Bruker AvanceCore spectrometer operating at 400 MHz for ^1H and 100 MHz for ^{13}C. High-resolution mass spectrometry (HRMS) measurements were conducted using electrospray ionization (Bruker Daltonics Corporation, Q-TOF geometry impact II). Infrared (IR) spectra were recorded on a Frontier spectrometer with an attenuated total reflectance (ATR) accessory (PerkinElmer, Waltham, USA). Melting points were determined using a digital melting point apparatus (MQAPF-302, Microquímica Equipamentos, Brazil). NMR, MS, and IR spectra for all synthesized compounds are provided as supplementary material.

Synthesis of Furfural and 5-Hydroxymethylfurfural

FF and HMF were synthesized according to methodologies previously described.[64,65] Briefly, for the synthesis of FF, 0.25 mmol of D-xylose, 1.0 mL of saturated aqueous NaCl solution, 1.0 mol% of $CX4SO_3H$, and 3.0 mL of butyl acetate were combined in a Pyrex glass tube. The mixture was placed in the MWI reactor cavity and heated at 160 °C for 10 min, utilizing a maximum power of 150 W. Following this, the organic phase was separated, dried over anhydrous sodium sulfate, filtered, and the solvent was removed under reduced pressure using a rotary evaporator.[64]

For the synthesis of HMF, 0.25 mmol of D-fructose, 1.0 mL of saturated aqueous NaCl solution, 1.0 mol% of $CX4SO_3H$, and 4.0 mL of ethyl acetate were combined in a Pyrex glass tube. The reaction mixture was placed in the MWI reactor cavity and heated at 140 °C for 10 min, using a maximum power of 75 W. The organic phase was then separated, dried over anhydrous sodium sulfate, filtered, and concentrated under reduced pressure using a rotary evaporator.[65]

Spectroscopy Data of FF and HMF: FF

Yellow liquid, yield 77%. IR (cm^{-1})$\bar{\nu}_{max}$: 3134, 2849, 2814, 1671, 1567, 1468, 1397, 1278, 1019, 930, and 748. GC–MS (*m/z*) (abundance %): 96 (100, M^+), 95 (98), 67 (15), 51 (3). ^1H NMR ($CDCl_3$, 300 MHz): δ 6.57 (dd, $J = 3.6$ Hz and $J = 1.7$ Hz, 1 H, H-Furan), 7.22 (dd, $J = 3.6$ Hz and $J = 0.8$ Hz, 1 H, H-Furan), 7.66 (m, 1 H, H-Furan), 9.62 (s, 1 H, CHO). ^{13}C NMR ($CDCl_3$, 75 MHz) δ 177.8, 152.9, 148.0, 121.0, 112.5.

Spectroscopy Data of FF and HMF: HMF

Yellow liquid, yield 74%. IR (cm^{-1}) $\bar{\nu}_{max}$: 3336, 2931, 2837, 1659, 1513, 1395, 1186, 1111, 764. GC–MS (*m/z*) (abundance %): 126 (55, M^+), 97 (100), 69 (35), 41 (65). ^1H NMR ($CDCl_3$, 300 MHz) δ 4.68 (s, 2 H, $HOCH_2$), 6.49 (d, $J = 3.6$ Hz, 1 H, H-Furan), 7.20 (d, $J = 3.6$ Hz, 1 H, H-Furan), 9.53 (s, 1 H, CHO). ^{13}C NMR ($CDCl_3$, 75 MHz) δ 57.4, 110.0, 123.3, 152.2, 160.9, 177.7.

Evaluation of Reaction Parameters for the Synthesis of Dihydropyridines, Sample Preparation and Analysis

The effects of reaction parameters—time, catalyst load, and temperature—on the synthesis of dihydropyridines were assessed using the following reaction model: 1.0 mmol of FF, 2.0 mmol of ammonium acetate, 2.0 mmol of ethyl acetoacetate, and $CX4SO_3H$ were combined in a Pyrex glass tube. The mixture was then placed in the MWI reactor under a maximum power of 100 W. At the conclusion of each experiment, the system was cooled to room temperature, yielding a yellow solid as the reaction product. Subsequently, 500 μL of saturated aqueous NaCl solution and 2.0 mL of ethyl acetate were added to the tube. The mixture was stirred until the solid was completely dissolved and allowed to rest for phase separation. The organic phase was then removed, and a second liquid–liquid extraction was performed with an additional 2.0 mL of ethyl acetate. The organic phases were combined, and any residual water was removed with anhydrous sodium sulphate. This mixture was filtered, transferred to a round-bottom flask, and the ethyl acetate was evaporated under reduced pressure using a rotary evaporator.

The obtained dihydropyridine was quantified using an external calibration technique, with TMB as the internal standard, according to a methodology reported by Castro and Fernandes,[65] with minor modifications. Specifically, 6.25 mg of the of the dry reaction mixture was transferred to a 5.00 mL volumetric flask, which was then filled with a solution of 1,3,5-trimethoxybenzene (TMB) at 1.00 mg mL^{-1}. After homogenization, the solution was analyzed by GC–MS under the following experimental parameters: column SBP-5, 30 m, ID 0.25 mm; helium as the carrier gas; injector temperature: 290 °C; oven temperature: 40 °C (for 2 min), ramping at 20 °C min^{-1} to 300 °C (held for 5 min); and injection volume: 1 μL. Standard solutions of the dihydropyridine were prepared at concentrations ranging from 0.20 to 1.25 mg mL^{-1} in ethyl acetate, keeping TMB concentration fixed at 1.00 mg mL^{-1}. Then, 1 μL of each standard solution was injected into the GC–MS system. The calibration curve ($R^2 = 0.9986$) was established based on the ratio of the dihydropyridine area to the TMB area for each injected standard. The concentration of dihydropyridine was calculated using this calibration curve (ESI, Figure S9, Supporting Information), and the reaction yield was determined using Equation (1), where *n* corresponds to the number of moles.

$$\text{Yield of dihydropyridine}\,(\%) = \frac{n_{\text{dihydropyridine}}}{n_{\text{furfural}}} \cdot 100 \quad (1)$$

Research Article
doi.org/10.1002/ejoc.202500278

Synthesis of Dihydropyridines

For the synthesis of dihydropyridines (**D1–D21**), 1.0 mmol of the furanic compound, 2.0 mmol of ammonium acetate, 2.0 mmol of ethyl or methyl acetoacetate, and 1.0 mol% of $CX4SO_3H$ were combined in a Pyrex glass tube. The mixture was then placed in the MWI reactor, and the reaction was conducted at 80 °C for 10 min, with a maximum power of 100 W. After this, the tube was removed from the reactor cavity and allowed to cool to room temperature, yielding a solid product corresponding to the dihydropyridines. For purification, this solid was completely dissolved in a minimum amount of hot ethanol. Subsequently, 10 mL of ice-cold distilled water was added to this solution, resulting in the precipitation of the dihydropyridine. The obtained precipitate was then filtered under vacuum, washed with cold distilled water, and allowed to dry in a vacuum. The reaction yields were calculated using Equation (1), where *n* represents the number of moles of the furanic compound used as the starting material and the corresponding dihydropyridine.

Spectroscopy Data of Synthesized Dihydropyridines (D1–D21): Diethyl 4-(furan-2-yl)-2,6-Dimethyl-1,4-Dihydropyridine-3,5-Dicarboxylate (D1)

Yellow solid, yield 96%. M.p. 162.5−63.4 °C. IR (cm^{-1}) $\bar{\nu}_{max}$: 3344, 2986, 1697, 1648, 1489, 1370, 1203, 1096, 1008, 807, 730. GC–MS (m/z) (abundance %): 319 (21, M^+), 290 (17), 274 (12), 262 (17), 246 (100), 218 (16), 202 (15), 200 (9), 174 (9), 150 (5). ^1H NMR (300 MHz, $CDCl_3$) δ 1.26 (t, $J = 7.0$ Hz, 6 H, CH_3), 2.32 (s, 6 H, CH_3), 4.10–4.22 (m, 4 H, OCH_2), 5.19 (s, 1 H, CH), 5.80 (s, 1 H, NH), 5.94 (d, $J = 3.2$ Hz, 1 H, H-furan), 6.20 (dd, $J = 3.2$ Hz and $J = 1.9$ Hz, 1 H, H-furan), 7.20–7.21 (m, 1 H, H-furan). ^{13}C NMR (75 MHz, $CDCl_3$) δ 14.3, 19.5, 33.4, 59.8, 100.7, 104.4, 110.0, 140.8, 145.0, 158.7, 167.4.

Spectroscopy Data of Synthesized Dihydropyridines (D1–D21): Dimethyl 4-(furan-2-yl)-2,6-Dimethyl-1,4-Dihydropyridine-3,5-Dicarboxylate (D2)

Yellow solid, yield 89%. M.p. 189.7–190.3 °C. IR (cm^{-1}) $\bar{\nu}_{max}$: 3346, 2995, 2952, 1699, 1644, 1489, 1203, 1121, 1096, 1009, 807, 730. GC–MS (m/z) (abundance %): 291 (22, M^+), 276 (10), 260 (12), 232 (100), 200 (21), 192 (7), 172 (8), 144 (5). ^1H NMR (400 MHz, $CDCl_3$) δ 2.33 (s, 1 H, CH_3), 3.70 (s, 6 H CH_3), 5.19 (s, 1 H, CH), 5.89 (s, 1 H, NH), 5.92 (d, $J = 3.2$ Hz, 1 H, H-furan), 6.20 (dd, $J = 3.2$ Hz and $J = 1.4$ Hz, 1 H, H-furan), 6.7.20–7.21 (m, 1 H, H-furan). ^{13}C NMR (100 MHz, $CDCl_3$) δ 19.5, 33.3, 51.2, 100.5, 104.3, 110.0, 145.5, 158.4, 167.9.

Spectroscopy Data of Synthesized Dihydropyridines (D1–D21): Diethyl 2,6-Dimethyl-4-(5-Methylfuran-2-Yl)-1,4-Dihydropyridine-3,5-Dicarboxylate (D3)

Yellow solid, yield 78%. M.p. 142.5–142.7 °C. IR (cm^{-1}) $\bar{\nu}_{max}$: 3336, 3248, 3111, 2994, 1697, 1652, 1492, 1372, 1307, 1207, 1124, 1092, 1017, 778. GC–MS (m/z) (abundance %): 333 (47, M^+), 304 (35), 288 (15), 276 (17), 260 (100), 232 (23), 214 (33), 196 (10). ^1H NMR (400 MHz, $CDCl_3$) δ 1.26 (t, $J = 7.0$ Hz, 6 H, CH_3), 2.18 (s, 3 H, CH_3-Furan), 2.31 (s, 6 H, CH_3), 4.09–4.24 (m, 4 H, OCH_3), 5.12 (s, 1 H, CH), 5.76 (s, 2 H, H-furan), 5.81 (s, 1 H, NH). ^{13}C NMR (100 MHz, $CDCl_3$) δ 13.7, 14.4, 19.5, 33.4, 59.7, 100.9, 105.0, 105.8, 144.8, 150.3, 157.0, 167.6.

Spectroscopy Data of Synthesized Dihydropyridines (D1–D21): Dimethyl 2,6-Dimethyl-4-(5-Methylfuran-2-Yl)-1,4-Dihydropyridine-3,5-Dicarboxylate (D4)

Yellow solid, yield 87%. M.p. 181.6–182.6 °C. IR (cm^{-1}) $\bar{\nu}_{max}$: 3348, 3004, 2953, 1695, 1652, 1492, 1436, 1344, 1304, 1210, 1123, 1016, 774, 748. GC–MS (m/z) (abundance %): 305 (44, M^+), 290 (20), 274 (17), 246 (100), 224 (22), 214 (42), 204 (16). ^1H NMR (300 MHz, $CDCl_3$) δ 2.18 (s, 3 H, CH_3-Furan), 2.32 (s, 6 H, CH_3), 3.70 (s, 6 H, OCH_3), 5.12 (s, 1 H, CH), 5.77 (s, 2 H, H-furan), 5.87 (s, 1 H, NH). ^{13}C NMR (75 MHz, $CDCl_3$) δ 13.7, 19.5, 33.2, 51.1, 100.7, 104.9, 105.9, 145.3, 150.5, 156.6, 168.

Spectroscopy Data of Synthesized Dihydropyridines (D1–D21): Diethyl 4-(5-(Hydroxymethyl)Furan-2-yl)-2,6-Dimethyl-1,4-Dihydropyridine-3,5-Dicarboxylate (D5)

Yellow solid, yield 81%. M.p. 145.4–146.6 °C. IR (cm^{-1}) $\bar{\nu}_{max}$: 3425, 3274, 3230, 3105, 2985, 2927, 1683, 1625, 1494, 1382, 1281, 1205, 1108, 1010, 784. GC–MS (m/z) (abundance %): 349 (15, M^+), 331 (20), 304 (14), 276 (100), 248 (18), 230 (20), 202 (15), 186 (18). ^1H NMR (300 MHz, $CDCl_3$) δ 1.26 (t, $J = 7.1$ Hz, 3 H, CH_3), 2.29 (s, 6 H, CH_3), 4.07–4.24 (m, 4 H, OCH_2), 4.46 (s, 2 H, CH_2-Furan), 5.16 (s, 1 H, CH), 5.86 (d, $J = 3.7$ Hz, 1 H, H-Furan), 6.06–6.10 (m, 2 H, NH and H-Furan). ^{13}C NMR (75 MHz, $CDCl_3$) δ 14.3, 19.4, 33.5, 57.6, 59.8, 100.4, 106.3, 108.5, 145.3, 152.3, 158.9, 167.6.

Spectroscopy Data of Synthesized Dihydropyridines (D1–D21): Dimethyl 4-(5-(Hydroxymethyl)Furan-2-yl)-2,6-Dimethyl-1,4-Dihydropyridine-3,5-Dicarboxylate (D6)

Yellow solid, yield 94%. M.p. 142.2–144.0 °C. IR (cm^{-1}) $\bar{\nu}_{max}$: 3353, 3112, 2999, 2953, 2845, 1700, 1651, 1490, 1429, 1339, 1209, 1115, 1017, 797, 740. GC–MS (m/z) (abundance %): 321 (20, M^+), 303 (27), 290 (28), 262 (100), 230 (20), 224 (32), 192 (17). ^1H NMR (300 MHz, $CDCl_3$) δ 2.29 (s, 6 H, CH_3), 3.69 (s, 6 H, OCH_3), 4.46 (s, 2 H, CH_2-Furan), 5.15 (s, 1 H, CH), 5.85 (d, $J = 3.1$ Hz, 1 H, H-Furan), 6.09 (d, $J = 3.1$ Hz, 1 H, H-Furan), 6.22 (s, 1 H, NH). ^{13}C NMR (75 MHz, $CDCl_3$) δ 19.3, 33.4, 51.1, 57.5, 100.1, 105.2, 108.5, 145.8, 152.5, 158.6, 168.0.

Spectroscopy Data of Synthesized Dihydropyridines (D1–D21): Dimethyl 4-(5-Ethylfuran-2-yl)-2,6-Dimethyl-1,4-Dihydropyridine-3,5-Dicarboxylate (D7)

Yellow solid, yield 86%. M.p. 157.1–157.8 °C. IR (cm^{-1}) $\bar{\nu}_{max}$: 3338, 2974, 2950, 1701, 1652, 1485, 1430, 1343, 1297, 1213, 1118, 1102, 1014, 821, 803, 758. GC–MS (m/z) (abundance %): 319 (42, M^+), 304 (20), 288 (15), 260 (100), 228 (32), 224 (24), 204 (18). HRMS [ESI (+), Q-TOF] (m/z): $[M + Na]^+$ calculated for $NaC_{17}H_{21}NO_5$ 342.1312, found 342.1307. ^1H NMR (300 MHz, $CDCl_3$) δ 1.19 (t, $J = 7.5$ Hz, 3 H, CH_3), 2.32 (s, 6 H, OCH_3), 2.54 (q, $J = 7.5$ Hz, 2 H, CH_2-Furan), 3.71 (s, 6 H, CH_3), 5.13 (s, 1 H, CH), 5.77 (s, 2 H, H-Furan), 5.82 (s, 1 H, NH). ^{13}C NMR (75 MHz, $CDCl_3$) δ 11.8, 19.4, 33.2, 51.1, 100.7, 104.1, 104.6, 145.2, 156.1, 156.6, 168.0.

Spectroscopy Data of Synthesized Dihydropyridines (D1–D21): Diethyl 4-(4,5-Dimethylfuran-2-Yl)-2,6-Dimethyl-1,4-Dihydropyridine-3,5-Dicarboxylate (D8)

Yellow solid, yield 81%. M.p. 155.5–157.2 °C. IR (cm^{-1}) $\bar{\nu}_{max}$: 3334, 3102, 2983, 2935, 1691, 1652, 1491, 1295, 1208, 1097, 1049, 1024, 749. GC–MS (m/z) (abundance %): 347 (61, M^+), 318 (60), 290 (25), 274 (100), 246 (39), 228 (50). HRMS [ESI (+), Q-TOF] (m/z): $[M + Na]^+$ calculated for $NaC_{19}H_{25}NO_5$ 370.1624, found 370.1613. ^1H NMR (300 MHz, $CDCl_3$) δ 1.27 (t, $J = 7.1$ Hz, 3 H, CH_3), 1,83 (s, 3 H, CH_3-Furan), 2.08 (s, 3 H, CH_3-Furan), 2.32 (s, 6 H, CH_3), 4.08–4.26 (m, 4 H, OCH_2), 5.09 (s, 1 H, CH), 5.67 (s, 1 H, H-Furan), 5.77 (s, 1 H, NH). ^{13}C NMR (75 MHz, $CDCl_3$) δ 10.0, 11.4, 14.3, 19.5, 33.2, 59.7, 101.0, 107.6, 114.1, 144.7, 145.5, 155.6, 167.6.

Spectroscopy Data of Synthesized Dihydropyridines (D1–D21): Dimethyl 4-(4,5-Dimethylfuran-2-Yl)-2,6-Dimethyl-1,4-Dihydropyridine-3,5-Dicarboxylate (D9)

Yellow solid, yield 81%. M.p. 207.7–208.9 °C. IR (cm^{-1}) $\bar{\nu}_{max}$: 3344, 3108, 2957, 2920, 1693, 1651, 1488, 1434, 1342, 1213, 1124, 1018, 823, 747. GC–MS (m/z) (abundance %): 319 (65, M^+), 304 (32), 288 (17), 260 (100), 228 (46), 224 (26). HRMS [ESI (+), Q-TOF] (m/z): $[M + Na]^+$ calculated for $NaC_{17}H_{21}NO_5$ 342.1312, found 342.1307. ^{1}H NMR (300 MHz, $CDCl_3$) δ 1.83 (s, 3 H, CH_3-Furan), 2.08 (s, 3 H, CH_3-Furan), 2.32 (s, 6 H, CH_3), 3.71 (s, 6 H, OCH_3), 5.08 (s, 1 H, CH), 5.67 (s, 1 H, H-Furan), 5.84 (s, 1 H, NH). ^{13}C NMR (75 MHz, $CDCl_3$) δ 9.9, 11.4, 19.5, 33.1, 51.1, 100.7, 107.5, 114.2, 145.2, 145.7, 155.3, 168.0.

Spectroscopy Data of Synthesized Dihydropyridines (D1–D21): Diethyl 4-(5-(4-Chlorophenyl)Furan-2-yl)-2,6-Dimethyl-1,4-Dihydropyridine-3,5-Dicarboxylate (D10)

Yellow solid, yield 87%. M.p. 183.6–185.6 °C. IR (cm^{-1}) $\bar{\nu}_{max}$: 3323, 3245, 3102, 2984, 1684, 1643, 1481, 1372, 1204, 1091, 1017, 835, 782. GC–MS (m/z) (abundance %): 431 (15, M^{+2}), 429 (46, M^+), 400 (66), 372 (23), 356 (100), 328 (24), 310 (36), 196 (22), 178 (21), 139 (47). ^{1}H NMR (400 MHz, $CDCl_3$) δ 1.30 (t, $J = 7.1$ Hz, 6 H, CH_3), 2.27 (s, 6 H, CH_3), 4.14–4.28 (m, 4 H, OCH_2), 5.26 (s, 1 H, CH), 5.93 (s, 1 H, NH), 6.03 (s, 1 H, H-Furan), 6.90 (s, 1 H, H-Furan), 7.30 (d, $J = 8.7$ Hz, 2 H, H-Ar), 7.30 (d, $J = 8.7$ Hz, 2 H, H-Ar). ^{13}C NMR (100 MHz, $CDCl_3$) δ 14.4, 19.5, 33.6, 59.9, 100.6, 106.3, 106.8, 124.5, 128.7, 129.9, 132.1, 145.3, 151.0, 159.0, 167.4.

Spectroscopy Data of Synthesized Dihydropyridines (D1–D21): Dimethyl 4-(5-(4-Chlorophenyl)Furan-2-yl)-2,6-Dimethyl-1,4-Dihydropyridine-3,5-Dicarboxylate (D11)

Yellow solid, yield 91%. M.p. 210.6–212.6 °C. IR (cm^{-1}) $\bar{\nu}_{max}$: 3319, 3110, 2991, 2949, 1705, 1655, 1481, 1435, 1344, 1300, 1210, 1119, 1016, 808, 774, 753. GC–MS (m/z) (abundance %): 403 (13, M^{+2}), 401 (39, M^+), 386 (33), 370 (13), 342 (100), 310 (34), 224 (31), 192 (13), 165 (23), 139 (38). ^{1}H NMR (300 MH z, $CDCl_3$) δ 2.36 (s, 6 H, CH_3), 3.74 (s, 6 H, OCH_3), 5.24 (s, 1 H, CH), 5.90 (s, 1 H, NH), 5.99 (d, $J = 3.3$ Hz, 1 H, H-Furan), 6.47 (d, $J = 3.3$ Hz, 1 H, H-Furan), 7.28 (d, $J = 8.7$ Hz, 2 H, H-Ar), 7.44 (d, $J = 8.7$ Hz, 2 H, H-Ar). ^{13}C NMR (75 MHz, $CDCl_3$) δ 19.5, 33.4, 51.2, 100.3, 106.2, 106.6, 124.5, 128.7, 129.9, 132.2, 145.6, 151.1, 158.6, 167.8.

Spectroscopy Data of Synthesized Dihydropyridines (D1–D21): Diethyl 4-(5-(2-Chlorophenyl)Furan-2-yl)-2,6-Dimethyl-1,4-Dihydropyridine-3,5-Dicarboxylate (D12)

Yellow solid, yield 92%. M.p. 138.8–140.6 °C. IR (cm^{-1}) $\bar{\nu}_{max}$: 3343, 2990, 1690, 1655, 1470, 1367, 1203, 1109, 1021, 810, 743. GC–MS (m/z) (abundance %): 431 (11, M^{+2}), 429 (32, M^+), 400 (43), 372 (16), 356 (100), 328 (19), 310 (20), 196 (18), 178 (17), 139 (37). ^{1}H NMR (300 MHz, $CDCl_3$) δ 1.28 (t, $J = 7.1$ Hz, 6 H, CH_3), 2.35 (s, 6 H, CH_3), 4.14–1.25 (m, 4 H, OCH_2), 5.27 (s, 1 H, CH), 5.90 (s, 1 H, NH), 6.07 (d, $J = 3.4$ Hz, 1 H, H-Furan), 6.98 (d, $J = 3.4$ Hz, 1 H, H-Furan), 7.11 (dt, $J = 7.6$ Hz and $J = 1.8$ Hz, 1 H, H-Ar), 7.22 (d, $J = 7.8$ Hz, 1 H, H-Ar), 7.37 (d, $J = 8.0$ Hz, 1 H, H-Ar), 7.72 (dd, $J = 8.0$ Hz and $J = 1.8$ Hz, 1 H, H-Ar). ^{13}C NMR (75 MHz, $CDCl_3$) δ 14.4, 19.5, 33.5, 59.9, 100.6, 106.7, 111.8, 126.6, 127.2, 127.3, 129.5, 129.5, 130.6, 145.3, 148.3, 158.5, 167.4.

Spectroscopy Data of Synthesized Dihydropyridines (D1–D21): Dimethyl 4-(5-(2-Chlorophenyl)Furan-2-yl)-2,6-Dimethyl-1,4-Dihydropyridine-3,5-Dicarboxylate (D13)

Yellow solid, yield 89%. M.p. 207.0–208.9 °C. IR (cm^{-1}) $\bar{\nu}_{max}$: 3324, 2959, 1704, 1654, 1488, 1433, 1340, 1296, 1216, 1122, 1018, 748. GC–MS (m/z) (abundance %): 403 (11, M^{+2}) 401 (32, M^+), 386 (23), 342 (100), 310 (28), 224 (24), 139 (34). ^{1}H NMR (300 MHz, $CDCl_3$) δ 2.35 (s, 6 H, CH_3), 4.74 (s, 6 H, OCH_3), 5.26 (s, 1 H, CH), 5.96 (s, 1 H, NH), 6.05 (d, $J = 3.4$ Hz, 1 H, H-Furan), 6.97 (d, $J = 3.4$ Hz, 1 H, H-Furan), 7.11 (dt, $J = 7.4$ Hz and $J = 1.7$ Hz, 1 H, H-Ar), 7.23 (dd, $J = 7.8$ Hz and $J = 1.4$ Hz, 1 H, H-Ar), 7.37 (d, $J = 8.0$ Hz, 1 H, H-Ar), 7.69 (dd, $J = 7.9$ Hz and $J = 1.7$ Hz, H-Ar). ^{13}C NMR (75 MHz, $CDCl_3$) δ 19.5, 33.4, 51.2, 100.3, 106.5, 111.8, 126.7, 127.3, 129.5, 129.5, 130.6, 145.7, 148.5, 158.2, 167.8.

Spectroscopy Data of Synthesized Dihydropyridines (D1–D21): Diethyl 4-(5-(4-Bromophenyl)Furan-2-yl)-2,6-Dimethyl-1,4-Dihydropyridine-3,5-Dicarboxylate (D14)

Yellow solid, yield 94%. M.p. 169.4–171.3 °C. IR (cm^{-1}) $\bar{\nu}_{max}$: 3324, 3094, 2982, 1687, 1644, 1477, 1371, 1199, 1124, 1094, 1019, 780. GC–MS (m/z) (abundance %): 475 (47, M^{+2}), 473 (48, M^+), 446 (70), 418 (20), 402 (100), 372 (24), 356 (37), 252 (20), 224 (25), 196 (35), 183 (34), 150 (25). ^{1}H NMR (300 MHz, $CDCl_3$) δ 1.27 (t, $J = 7.1$ Hz, 6 H, CH_3), 2.35 (s, 6 H, CH_3), 4.13–4.24 (m, 4 H, OCH_3), 5.23 (s, 1 H, CH), 5.83 (s, 1 H, NH), 6.01 (d, $J = 3.3$ Hz, 1 H, H-Furan), 6.49 (d, $J = 3.3$ Hz, 1 H, H-Furan), 7.37–7.45 (m, 4 H, H-Ar). ^{13}C NMR (75 MHz, $CDCl_3$) δ 14.4, 19.5, 36.6, 59.9, 100.6, 106.4, 106.8, 120.2, 124.7, 130.3, 131.6, 145.2, 150.9, 159.1, 167.4.

Spectroscopy Data of Synthesized Dihydropyridines (D1–D21): Dimethyl 4-(5-(4-Bromophenyl)Furan-2-yl)-2,6-Dimethyl-1,4-Dihydropyridine-3,5-Dicarboxylate (D15)

Yellow solid, yield 90%. M.p. 220.7–222.0 °C. IR (cm^{-1}) $\bar{\nu}_{max}$: 3320, 3250, 3109, 2950, 1706, 1656, 1477, 1435, 1344, 1212, 1120, 1016, 808, 774, 753. GC–MS (m/z) (abundance %): 447 (39, M^{+2}), 445 (38, M^+), 386 (100), 354 (38), 224 (55), 207 (36), 183 (34), 165 (40), 44 (40). ^{1}H NMR (300 MHz, $CDCl_3$) δ 2.36 (s, 6 H, CH_3), 3.74 (s, 6 H, CH_3), 5.23 (s, 1 H, CH), 5.88 (s, 1 H, NH), 5.99 (d, $J = 3.3$ Hz, 1 H, H-Furan), 6.48 (d, $J = 3.3$ Hz, 1 H, H-Furan), 7.36–7.45 (m, 4 H, H-Ar). ^{13}C NMR (75 MHz, $CDCl_3$) δ 19.5, 33.4, 51.2, 100.3, 106.3, 106.6, 120.3, 124.7, 130.2, 131.6, 145.6, 151.1, 158.6, 167.8.

Spectroscopy Data of Synthesized Dihydropyridines (D1–D21): Diethyl 2,6-Dimethyl-4-(5-(2-Nitrophenyl)Furan-2-Yl)-1,4-Dihydropyridine-3,5-Dicarboxylate (D16)

Yellow solid, yield 95%. M.p. 142.0–144.0 °C. IR (cm^{-1}) $\bar{\nu}_{max}$: 3346, 2989, 1689, 1655, 1522, 1472, 1366, 1200, 1109, 1023, 740. GC–MS (m/z) (abundance %): 440 (15, M^+), 423 (13), 395 (12), 367 (100), 252 (23), 204 (16), 196 (28), 178 (17), 150 (20). ^{1}H NMR (300 MHz, $CDCl_3$) δ 1.27 (t, $J = 7.1$ Hz, 6 H, CH_3), 2.36 (s, 6 H, CH_3), 4.11–4.21 (m, 4 H, OCH_2), 5.14 (s, 1 H, CH), 6.03 (s, 1 H, NH), 6.12 (d, $J = 3.3$ Hz, 1 H, H-Furan), 6.58 (d, $J = 3.3$ Hz, 1 H, H-Furan), 7.28 (t, $J = 7.8$ Hz, 1 H, H-Furan), 7.43–7.51 (m, 2 H, H-Ar), 7.57 (d, $J = 8.0$ Hz, 1 H, H-Ar). ^{13}C NMR (75 MHz, $CDCl_3$) δ 14.3, 19.5, 33.4, 59.8, 99.7, 106.4, 110.2, 123.6, 123.8, 127.2, 127.5, 131.3, 146.0, 146.5, 160.5, 167.2.

Spectroscopy Data of Synthesized Dihydropyridines (D1–D21): Dimethyl 2,6-Dimethyl-4-(5-(2-Nitrophenyl)Furan-2-Yl)-1,4-Dihydropyridine-3,5-Dicarboxylate (D17)

Yellow solid, yield 92%. M.p. 176.0–178.0 °C. IR (cm^{-1}) $\bar{\nu}_{max}$: 3334, 2950, 1696, 1665, 1529, 1439, 1369, 1212, 1103, 1017, 782, 751, 689. GC–MS (m/z) (abundance %): 412 (16, M^+), 395 (14), 381 (13), 363 (18), 353 (100), 292 (14), 249 (17), 224 (70), 207 (28), 192 (48), 179 (20), 164 (23), 77 (26). ^{1}H NMR (300 MHz, $CDCl_3$) δ 2.36

(s, 6 H, CH_3), 3.71 (s, 6 H, CH_3), 5.13 (s, 1 H, CH), 6.08 (s, 1 H, NH), 6.11 (d, $J = 3.3$ Hz, 1 H, H-Furan), 6.57 (d, $J = 3.3$ Hz, 1 H, H-Furan), 7.30 (d, $J = 7.9$ Hz, H-Ar), 7.44–7.52 (m, 2 H, H-Ar), 7.56 (d, $J = 7.9$ Hz, H-Ar). ^{13}C NMR (75 MHz, $CDCl_3$) δ 19.5, 33.3, 51.1, 99.6, 106.4, 110.2, 123.6, 123.7, 127.3, 127.6, 131.3, 146.3, 146.7, 160.3, 167.6.

Spectroscopy Data of Synthesized Dihydropyridines (D1–D21): Diethyl 2,6-Dimethyl-4-(5-((4-Methyl-4 H-1,2,4-Triazol-3-Yl)Thio)Furan-2-Yl)-1,4-Dihydropyridine-3,5-Dicarboxylate (D18)

Brown liquid, yield 60%. GC–MS (m/z) (abundance %): 432 (30, M^+), 359 (100), 244 (20), 216 (50). ^{1}H NMR (400 MHz, $CDCl_3$) δ 1.23 (t, $J = 7.2$ Hz, 6 H), 2.29 (s, 6 H), 3.70 (s, 3 H), 4.06–4.18 (m, 4 H), 5.14 (s, 1 H), 5.96 (d, $J = 3.3$ Hz, 1 H), 6.57 (d, $J = 3.3$ Hz, 1 H), 7.07 (s, 1 H), 8.19 (s, 1 H). ^{13}C NMR (100 MHz, $CDCl_3$) δ 14.3, 19.1, 31.8, 33.9, 59.8, 99.5, 107.1, 120.4, 136.0, 146.0, 146.2, 147.6, 163.5, 167.3.

Spectroscopy Data of Synthesized Dihydropyridines (D1–D21): Dimethyl 2,6-Dimethyl-4-(5-((4-Methyl-4 H-1,2,4-Triazol-3-Yl)Thio)Furan-2-Yl)-1,4-Dihydropyridine-3,5-Dicarboxylate (D19)

Brown solid, yield 43%. M.p. 154.1–156.0. GC–MS (m/z) (abundance %): 404 (35, M^+), 345 (100), 230 (40). ^{1}H NMR (400 MHz, $CDCl_3$) δ 2.29 (s, 6 H), 3.66 (s, 6 H), 3.71 (s, 3 H), 5.13 (s, 1 H), 5.94 (dd, $J = 3.1$ Hz e $J = 0.6$ Hz, 1 H), 6.56 (d, $J = 3.1$ Hz, 1 H), 7.23 (s, 1 H), 8.20 (s, 1 H). ^{13}C NMR (100 MHz, $CDCl_3$) δ 19.0, 31.8, 33.7, 99.1, 107.0, 120.3, 136.1, 146.0, 146.7, 147.6, 163.3, 167.7.

Spectroscopy Data of Synthesized Dihydropyridines (D1–D21): Diethyl 4-(5-(2-Bromo-4-Methylphenyl)Furan-2-yl)-2,6-Dimethyl-1,4-Dihydropyridine-3,5-Dicarboxylate (D20)

Yellow solid, yield 86%. M.p. 165.8–166.6 °C. GC–MS (m/z) (abundance %): 489 (47, M^{+2}), 487 (48, M^+), 458 (46), 414 (100). ^{1}H NMR (400 MHz, $CDCl_3$) δ 1.27 (t, $J = 7.1$ Hz, 6 H), 2.30 (s, 3 H), 2.34 (s, 6 H), 4.12–4.25 (m, 4), 5.25 (s, 1 H), 5.82 (s, 1 H), 6.04 (d, $J = 3.2$ Hz, 1 H), 6.94 (d, $J = 3.2$ Hz, 1 H), 7.09 (dd, $J = 8.1$ Hz e $J = 1.0$ Hz, 1 H), 7.41 (s, 1 H), 7.54 (d, $J = 8.0$ Hz, 1 H) .^{13}C NMR (100 MHz, $CDCl_3$) δ 14.4, 19.5, 20.6, 33.4, 59.9, 100.6, 106.3, 110.6, 118.8, 128.0, 128.1, 128.8, 134.4, 137.8, 145.2, 149.5, 158.2, 167.4.

Spectroscopy Data of Synthesized Dihydropyridines (D1–D21): Dimethyl 4-(5-(2-Bromo-4-Methylphenyl)Furan-2-yl)-2,6-Dimethyl-1,4-Dihydropyridine-3,5-Dicarboxylate (D21)

Yellow solid, yield 91%. M.p. 195.5–197.1 °C. GC–MS (m/z) (abundance %): 461 (45, M^{+2}), 459 (44, M^+), 400 (100), 207 (34). ^{1}H NMR (400 MHz, $CDCl_3$) δ 2.30 (s, 3 H), 2.35 (s, 6 H), 3.73 (s, 6 H), 5.24 (s, 1 H), 5.89 (s, 1 H), 6.02 (dd, $J = 3.4$ Hz e $J = 0.9$ Hz, 1 H), 6.93 (d, $J = 3.4$ Hz, 1 H), 7.09 (dd, $J = 8.0$ Hz e $J = 0.9$ Hz, 1 H), 7.42 (d, $J = 0.9$ Hz, 1 H), 7.52 (d, $J = 8.0$ Hz, 1 H).^{13}C NMR (100 MHz, $CDCl_3$) δ 19.5, 20.6, 33.3, 51.2, 100.3 106.1, 118.8, 128.0, 128.1, 128.7, 134.4, 137.9, 145.7, 149.7, 157.9, 167.8.

Reuse of $CX4SO_3H$

Organocatalyst recycling experiments were conducted using the afterward reaction model: 1.0 mmol of FF, 2.0 mmol of ammonium acetate, 2.0 mmol of ethyl acetoacetate, and 1.0 mol% of $CX4SO_3H$ were combined in a Pyrex glass tube and subjected to MWI irradiation at 80 °C for 10 min (using a maximum power of 100 W). Following this, the system was cooled to room temperature, and 2.0 mL of ethyl acetate was added to the reaction tube to facilitate the precipitation of $CX4SO_3H$. The mixture was then centrifuged, and the supernatant was removed for dihydropyridine quantification. $CX4SO_3H$ that had precipitated in the tube was washed with ethyl acetate (2×2.0 mL). The suspensions were centrifuged, the supernatants were discarded, and the tube was placed in an oven at 85 °C for 2 h to dry the $CX4SO_3H$. Subsequently, a new batch of FF (1.0 mmol), ammonium acetate (1.0 mmol), and ethyl acetoacetate (2.0 mmol) was added to the tube containing the recovered catalyst for a new reaction cycle. This process was repeated until a significant decrease in the yield of dihydropyridine was observed. After the final reuse cycle, the organocatalyst was precipitated and washed again with ethyl acetate, dried at 85 °C for 2 h, and then weighed.[32]

Single-Crystal X-ray Diffraction Technique

Single crystal X-ray diffraction data for structures of dihydropyridines **D12** and **D13** were collected on an Oxford Gemini A-Ultra diffractometer equipped with an Atlas CCD detector (Cu Kα radiation, 100 K). The Oxford programs CrysAlis CCD and CrysAlis RED[66] were used for cell refinement, data indexing, integration, and reduction. Multiscan absorption correction was performed for all datasets.[67] Structure solution was performed using SHELXL-2014[68] or SUPERFLIP[69] within WinGX.[70] All refinements were done with SHELXL.[68] Structure analysis and artwork preparation were applied with Mercury[71] and ORTEP-3.[72] Nonhydrogen and hydrogen atoms were refined anisotropically and isotropically, respectively. All CH hydrogens were added to their corresponding carbons following a riding model with fixed bond lengths and angles. Hydrogens had their isotropic atomic displacement parameters set to 1.2 Uiso of the corresponding carbon, except for methyl groups where this value was increased to 1.5. The complete X-ray diffraction dataset for all structures is available under CCDC number codes 2 353 476 (**D12**) and 2 353 481 (**D13**), which are shown in Table S1 (Supporting Information) along with a summary of the crystallographic data and refinement conditions.

Acknowledgements

The authors are thankful for the financial support provided by Fundação de Amparo à Pesquisa do Estado de Minas Gerais, Brazil (FAPEMIG), Conselho Nacional de Desenvolvimento Científico e Tecnológico, Brazil (CNPq), Coordenação de Aperfeiçoamento de Pessoal de Nível Superior, Brazil (CAPES - Finance Code 001), and Financiadora de Estudos e Projetos (FINEP). S.A.F. is supported by research fellowships from CNPq.

The Article Processing Charge for the publication of this research was funded by the Coordenação de Aperfeiçoamento de Pessoal de Nıvel Superior - Brasil (CAPES) (ROR identifier: 00x0ma614).

Conflict of Interest

The authors declare no conflict of interest.

Data Availability Statement

The data that support the findings of this study are available in the supplementary material of this article.

Keywords: 5-hydroxymethylfurfural · furfural · green chemistry · multicomponent reactions · *N*-heterocycles

[1] A. Ayvaz, S. G. Demirbaş, A. Demirbaş, N. Demirbaş, *Curr. Org. Chem.* **2023**, *27*, 585.
[2] A. Hantzsch, *Berichte der deutschen chemischen Gesellschaft* **1881**, *14*, 1637.
[3] A. Parthiban, P. Makam, *RSC Adv.* **2022**, *12*, 29253.
[4] A. Sarkar, P. P. Mondal, H. P. Nayek, *ChemistrySelect* **2020**, *5*, 12302.
[5] M. Schramm, G. Thomas, R. Towart, G. Franckowiak, *Nature* **1983**, *303*, 535.
[6] J. L. Reid, P. A. Meredith, F. Pasanisi, *J. Cardiovasc. Pharmacol.* **1985**, *7*, S18.
[7] K. K. Saini, R. Rani, Muskan, N. Khanna, B. Mehta, R. Kumar, *Curr. Org. Chem.* **2023**, *27*, 119.
[8] J. E. Arrowsmith, S. F. Campbell, P. E. Cross, J. K. Stubbs, R. A. Burges, D. G. Gardiner, K. J. Blackburn, *J. Med. Chem.* **1986**, *29*, 1696.
[9] S.-L. Boström, B. Ljung, S. Mårdh, S. Forsen, E. Thulin, *Nature* **1981**, *292*, 777.
[10] M. Iwanami, T. Shibanuma, M. Fujimoto, R. Kawai, K. Tamazawa, T. Takenaka, K. Takahashi, M. Murakami, *Chem. Pharm. Bull.* **1979**, *27*, 1426.
[11] M. C. Verhaar, M. L. H. Honing, T. van Dam, M. Zwart, H. A. Koomans, J. J. P. Kastelein, T. J. Rabelink, *Cardiovasc. Res.* **1999**, *42*, 752.
[12] X. H. Yang, P. H. Zhang, L. H. Hu, M. Zhang, C. G. Liu, H. J. Liu, Y. H. Zhou, *Ind. Crops Prod.* **2012**, *38*, 14.
[13] H. S. Sohal, *Mater. Today Proc.* **2022**, *48*, 1163.
[14] M. Faizan, R. Kumar, A. Mazumder, Salahuddin, N. Kukreti, P. K. Tyagi, B. Kapoor, *Synth. Commun.* **2024**, *54*, 1221.
[15] C. Castiello, P. Junghanns, A. Mergel, C. Jacob, C. Ducho, S. Valente, D. Rotili, R. Fioravanti, C. Zwergel, A. Mai, *Green Chem.* **2023**, *25*, 2109.
[16] R. A. Sheldon, *Green Chem.* **2017**, *19*, 18.
[17] H. N. Anchan, C. P. Naik, N. S. Bhat, M. Kumari, S. Dutta, *ACS Omega* **2023**, *8*, 34077.
[18] N. S. Bhat, M. Kumari, C. P. Naik, S. S. Mal, S. Dutta, *ChemistrySelect* **2023**, *8*, 202301782.
[19] J. Jiang, Y. Queneau, F. Popowycz, *ChemSusChem* **2024**, *17*, e202301782.
[20] G. A. D. Castro, S. A. Fernandes, *Sustain. Chem. Pharm.* **2025**, *44*, 101948.
[21] S. K. Brar, G. S. Dhillon, C. R. Soccol, *Biotransformation of Waste Biomass into High Value Biochemicals*, Springer, New York **2014**, p. 63.
[22] Q. Hou, X. Qi, M. Zhen, H. Qian, Y. Nie, C. Bai, S. Zhang, X. Bai, M. Ju, *Green Chem.* **2021**, *23*, 119.
[23] G. P. Perez, A. Mukherjee, M. J. Dumont, *J. Ind. Eng. Chem.* **2019**, *70*, 1.
[24] J. Y. Choi, J. Nam, B. Y. Yun, Y. U. Kim, S. Kim, *Ind. Crops Prod.* **2022**, *183*, 114931.
[25] G. A. D. Castro, S. A. Fernandes, R. de C. S. de Sousa, M. M. Pereira, *React Chem. Eng.* **2023**, *8*, 1324.
[26] N. R. Bocanegra, J. R. de la Rosa, C. J. L. Ortiz, P. C. González, H. C. Greenwell, V. E. B. Almaráz, L. S. Rangel, B. Alcántar-Vázquez, V. Rodríguez-González, D. A. de H. Del Río, *Catal. Today* **2021**, *360*, 2.
[27] G. A. D. Castro, S. A. Fernandes, *React Chem. Eng.* **2023**, *8*, 220.
[28] S. H. Shinde, C. V. Rode, *ACS Omega* **2018**, *3*, 5491.
[29] A. el-K. Sandeli, N. Khiri-Meribout, S. Benzerka, H. Boulebd, N. Gürbüz, N. Özdemir, İ. Özdemir, *New J. Chem.* **2021**, *45*, 17878.
[30] Ö. D. Ulu, *J. Mol. Struct.* **2021**, *1246*, 131202.
[31] C. D. Gutsche, *Calixarenes: An Introduction*, RSC Publishing, Arizona **2008**.
[32] G. A. D. Castro, S. A. Fernandes, *Sustain. Energy Fuels* **2021**, *5*, 108.
[33] G. A. D. Castro, A. Santos, A. G. Sathicq, V. Palermo, G. Romanelli, S. Fernandes, *React Chem. Eng.* **2022**, *7*, 2132.
[34] S. A. Fernandes, R. Natalino, M. J. da Silva, C. F. Lima, *Catal. Commun.* **2012**, *26*, 127.
[35] D. L. da Silva, S. A. Fernandes, A. A. Sabino, Â. de Fátima, *Tetrahedron Lett.* **2011**, *52*, 6328.
[36] J. B. Simões, D. L. da Silva, Â. de Fátima, S. A. Fernandes, *Curr. Org. Chem.* **2012**, *16*, 949.
[37] S. de P. S. Pereira, J. O. S. Varejão, Â. de Fátima, S. A. Fernandes, *Ind. Crops Prod.* **2019**, *138*, 111492.
[38] J. B. Simões, Â. de Fátima, A. A. Sabino, L. C. A. Barbosa, S. A. Fernandes, *RSC Adv.* **2014**, *4*, 18612.
[39] Y. L. Liu, L. Liu, Y. L. Wang, Y. C. Han, D. Wang, Y. J. Chen, *Green Chem.* **2008**, *10*, 635.
[40] W. F. de Paiva, Y. de F. Rego, Â. de Fátima, S. A. Fernandes, *Synthesis* **2022**, *54*, 3162.
[41] P. A. S. Abranches, W. F. de Paiva, Â. de Fátima, F. T. Martins, S. A. Fernandes, *J. Org. Chem.* **2018**, *83*, 1761.
[42] W. F. de Paiva, I. B. Braga, J. V. de Assis, S. M. B. Castañeda, Á. G. Sathicq, V. Palermo, G. P. Romanelli, R. Natalino, M. J. da Silva, F. T. Martins, G. S. G. de Carvalho, G. W. Amarante, S. A. Fernandes, *Tetrahedron* **2019**, *75*, 3740.
[43] T. R. M. Rezende, J. O. S. Varejão, A. L. L. de A. Sousa, S. M. B. Castañeda, S. A. Fernandes, *Org. Biomol. Chem.* **2019**, *17*, 2913.
[44] I. B. Braga, S. M. B. Castañeda, J. V. de Assis, A. O. Barros, G. W. Amarante, A. K. S. M. Valdo, F. T. Martins, A. F. do P. Rosolen, E. Pilau, S. A. Fernandes, *J. Org. Chem.* **2020**, *85*, 15622.
[45] V. Palermo, A. Sathicq, N. Liberto, S. Fernandes, P. Langer, J. Jios, G. Romanelli, *Tetrahedron Lett.* **2016**, *57*, 2049.
[46] S. Shimizu, N. Shimada, Y. Sasaki, *Green Chem.* **2006**, *8*, 608.
[47] J. B. Simões, D. L. da Silva, S. A. Fernandes, Â. de Fátima, *European J. Org. Chem.* **2022**, *2022*, e202200532.
[48] N. Sweygers, N. Alewaters, R. Dewil, L. Appels, *Sci. Rep.* **2018**, *8*, 1.
[49] Z. Fang, R. L. Smith Jr, X. Qi, *Production of Biofuels and Chemicals with Microwave*, Springer, Dordrecht **2015**.
[50] S. A. Fernandes, E. do C. Tavares, R. R. Teixeira, C. M. da Silva, R. M. Montanari, Â. de Fátima, C. P. A. Anconi, W. B. de Almeida, H. F. dos Santos, A. A. da Silva, *J. Incl. Phenom. Macrocycl. Chem.* **2013**, *75*, 197.
[51] R. Natalino, E. V. V. Varejão, M. J. da Silva, A. L. Cardoso, S. A. Fernandes, *Catal. Sci. Technol.* **2014**, *4*, 1369.
[52] C. Agarwal, A. K. Pandey, *Environ. Sci.: Adv.* **2023**, *2*, 1306.
[53] M. A. E. A. A. A. El-Remaily, H. A. Hamad, A. M. M. Soliman, O. M. Elhady, *Appl. Organomet. Chem.* **2021**, *35*, 6238.
[54] M. Bakhtiarian, M. M. Khodaei, *Mater. Today Commun.* **2021**, *29*, 102791.
[55] M. Shaibuna, K. Sreekumar, *Synth. Commun.* **2021**, *51*, 1742.
[56] P. Gupta, N. Prakash, Y. Ramawat, P. Rajput, A. Fayaz, T. K. Roy, *Lett. Org. Chem.* **2022**, *19*, 19.
[57] D. Ray, R. N. Yadav, B. K. Banik, *Results Chem.* **2022**, *4*, 100330.
[58] S. P. Patil, S. K. Shinde, M. U. Patil, S. S. Patil, *Res. Chem. Intermed.* **2022**, *48*, 3589.
[59] P. K. Singh, B. Khuntey, S. R. Bhardiya, M. Singh, V. K. Rai, A. Rai, *J. Heterocycl. Chem.* **2023**, *60*, 232.
[60] G. Kumar, G. Bhargava, R. Kumar, *Polycycl. Aromat. Compd.* **2023**, *43*, 7238.
[61] A. R. Katritzkr, D. L. Ostercamp, T. I. Yousaf, *Tetrahedrom* **1986**, *42*, 5729.
[62] V. G. Santos, M. N. , T. Regiani, F. H. S. Gama, M. B. Coelho, R. O. M. A. De Souza, M. N. Eberlin, S. J. Garden, *Chem. European J.* **2014**, *20*, 12808.
[63] J. Clayden, N. Greeves, S. Warren, P. Wothers, *Organic Chem*, Oxford University Press, New York **2000**.
[64] G. A. D. Castro, R. Batista, R. de C. S. de Sousa, A. de C. C. Carneiro, S. A. Fernandes, *React Chem. Eng.* **2023**, *8*, 1969.
[65] G. A. D. Castro, S. A. Fernandes, *Catal. Lett.* **2023**, *153*, 984.
[66] Rigaku Oxford Diffraction, *CrysAlisPRO*, https://rigaku.com/products/crystallography/X-ray-diffraction/crysalispro (accessed: November 2018).
[67] L. Krause, R. Herbst-Irmer, G. M. Sheldrick, D. Stalke, *J. Appl. Crystallogr.* **2015**, *48*, 3.
[68] G. M. Sheldrick, *Acta. Crystallogr. C Struct. Chem.* **2015**, *71*, 3.
[69] L. Palatinus, G. Chapuis, *J. Appl. Crystallogr.* **2007**, *40*, 786.
[70] L. J. Farrugia, *J. Appl. Crystallogr.* **1999**, *32*, 837.
[71] C. F. Macrae, I. J. Bruno, J. A. Chisholm, P. R. Edgington, P. McCabe, E. Pidcock, L. Rodriguez-Monge, R. Taylor, J. van de Streek, P. A. Wood, *J. Appl. Crystallogr.* **2008**, *41*, 466.
[72] L. J. Farrugia, *J. Appl. Crystallogr.* **1997**, *30*, 565.

Manuscript received: March 10, 2025
Revised manuscript received: June 16, 2025
Version of record online: July 10, 2025